

COMPUTING COMPLETE HYPERBOLIC STRUCTURES ON CUSPED 3-MANIFOLDS

CLÉMENT MARIA AND OWEN ROUILLÉ

ABSTRACT. A fundamental way to study 3-manifolds is through the geometric lens, one of the most prominent geometries being the hyperbolic one. We focus on the computation of a complete hyperbolic structure on a connected orientable hyperbolic 3-manifold with torus boundaries. This family of 3-manifolds include the knot complements.

This computation of a hyperbolic structure requires the resolution of gluing equations on a triangulation of the space, but not all triangulations admit a solution to the equations.

In this paper, we propose a new method to find a triangulation that admits a solution to the gluing equations, using convex optimization and combinatorial modifications. It is based on Casson and Rivin’s reformulation of the equations. We provide a novel approach to modify a triangulation and update its geometry, along with experimental results to support the new method.

1. INTRODUCTION

A main problem of knot theory is to tell whether two knots are equivalent or distinct. Equivalence between knots is defined by the existence of an isotopy of the ambient space that would turn one knot into the other, *i.e.*, a continuous deformation of the space that preserve the entanglements.

Isotopies are too difficult to compute in practice, and practitioners use *invariants* to tackle the knot equivalence problem. A *topological invariant* is a quantity assigned to a presentation of a knot and that is invariant by isotopy.

An important family of knots are the *hyperbolic knots*, which are the knots whose complements admit a *complete hyperbolic metric*. They are the subjects of active mathematical research, which motivates the introduction of efficient algorithmic tools to study their geometric properties, and most notably their *hyperbolic volume*. The hyperbolic volume of a hyperbolic knot is a topological invariant which is powerful at distinguishing between non-equivalent knots, is non-trivial to compute, and is at the heart of several deep conjectures in topology [9].

If it exists, the complete hyperbolic metric on a 3-manifold is unique[8], and they are combinatorially represented by *complete hyperbolic structures* (CHS). In order to compute geometric properties (such as volume) of a hyperbolic knot, one triangulates the knot complement, and try to assign hyperbolic shapes to its tetrahedra. If these *shapes* verify a set of non-linear constraints called the *gluing equations*, they form a CHS and encode the complete hyperbolic metric of the space. A major issue with this approach is that a solution to the constraints may not exist on all triangulations of a manifold, even if, as topological object, the manifold can carry a complete hyperbolic metric. Worst, it is not known whether every hyperbolic 3-manifold admits a triangulation on which a solution as CHS exists.

Key words and phrases. knots and 3-manifolds, triangulations, hyperbolic structure, Thurston equations.

INRIA Sophia Antipolis-Méditerranée, clement.marie@inria.fr, owen.rouille@inria.fr. This work has been partially supported by the ANR project ANR-20-CE48-0007-01 (AlgoKnot).

#crossings	Alternating						Non-Alternating					
	12	13	14	15	16	17	12	13	14	15	16	17
% Failure on first try	0.9	1.6	2.4	3.3	4.4	5.7	0.8	0.7	1.2	1.7	2.4	3.3
Expected nb of retriang.	2.9	3.9	6.2	7.1	9.5	15.9	2.0	3.1	6.1	11.8	9.7	13.5

FIGURE 1. On all ~ 9.7 millions prime knots with crossing numbers ranging from 12 to 17, alternating and non-alternating, we indicate (*% Failure on first try*) the percentage of knot complements (after triangulation and simplification) on which **SnapPy** fails to compute a CHS on first try. We also indicate (*Highest expected nb of retriang.*) the highest, over all knots, expected number of random re-triangulations necessary for **SnapPy** to succeed finding a CHS.

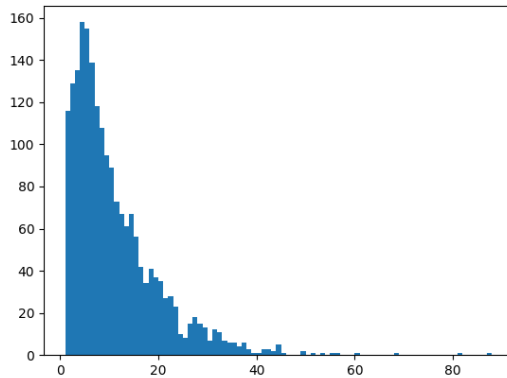


FIGURE 2. Distribution of the number of randomizations required to find a CHS for the complement of the knot “17nh_2654001” of the census, for 2000 tries. The mean is 10.6 randomizations, and the standard deviation is 9.0. The minimum number of re-triangulations is 1, and the maximum 88.

In practice, given an input knot, software can construct and simplify a triangulation of the knot complement that admits a CHS with high probability. But if the triangulation does not admit a CHS, the only implemented practical solution, proposed by **SnapPy**[3], is to randomly modify and simplify the triangulation before trying again until a CHS is found.

Figure 1 provides data on the search for a CHS with **SnapPy**, on the ~ 9.7 millions prime knots with crossing numbers up to 17. As observed, **SnapPy** has a high rate of success in finding a CHS after a standard triangulation and simplification of the knot complement. However, this standard construction of a triangulation fails to admit a CHS on more than 350 millions knots in the census, and the percentage of problematic triangulations needing re-triangulations, tends to increase with the number of crossings. Additionally, we observe that some knot complements may require in expectation a high number of random re-triangulations (up to 15.9), and the number of re-triangulations may itself suffer a high variance, as illustrated in Figure 2.

Checking for the existence of a CHS is a costly procedure, that requires the resolution of the non-linear gluing equations (with e.g. Newton optimization method). Reducing the number of re-triangulation is consequently critical for performance of computation in knot theory, most notably for knots on which the state-of-the-art methods implemented in **SnapPy**

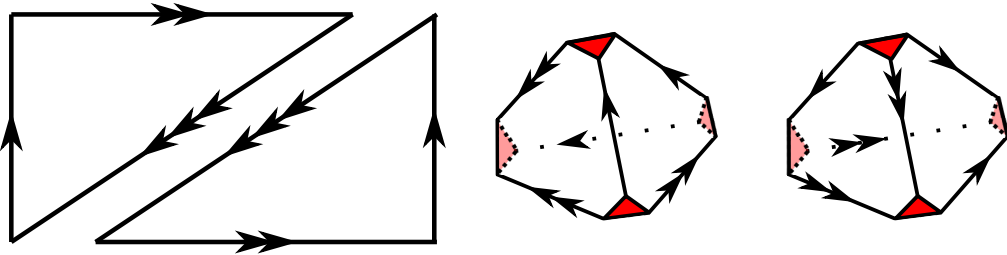


FIGURE 3. Left: 2-dimensional triangulation of the torus with two triangles. The edges are glued with respect to the arrows. Right: ideal triangulation of the complement of the 8-knot with two tetrahedra. The ideal vertex is truncated, and the red surface gives the torus link of the ideal vertex after gluing of the tetrahedra following the edge identifications.

require large numbers of re-triangulations, and even more so when proceeding to very large scale experiments such as the computation of the knot censuses [1] that are of great use to practitioners, where “difficult” knots are many.

Contribution: This paper introduces a new heuristic based algorithm to improve on the random approach. The method is inspired by Casson and Rivin’s reformulation of the gluing equations [13, 4]: the gluing equations are split into a linear part and a non-linear part, and the resolution reduces to a convex optimization problem on a polytope domain. If the triangulation does not admit a complete structure, the optimization problem will converge on the boundary of the polytope and we exploit this information to modify combinatorially the triangulation while reusing the partially computed geometry. We introduce necessary background on triangulations and geometry in Section 2, and the computation of hyperbolic structures with optimization in Section 3. We analyze precisely the behavior of the optimization phase on triangulation not admitting a CHS in Section 4, and introduce a re-triangulation algorithm in Section 5 guided by the partially computed geometry of the optimization phase. We illustrate experimentally the interest of the approach in Section 6 and propose a hybrid method with `SnapPy` in Section 7, that outperforms the state-of-the-art.

Note that, in this article we focus on complements of hyperbolic knots. However, the techniques introduced extend to more general hyperbolic 3-manifold with torus boundaries.

2. BACKGROUND

In this article, we focus on knot complements, *i.e.*, non-compact 3-manifolds obtained by removing a closed regular neighborhood of a knot K in S^3 . We denote such manifold by $S^3 \setminus K$.

2.1. Generalized and ideal triangulations. A *generalized triangulation* T is a collection of n abstract tetrahedra whose triangular facets are identified, or *glued*, in pairs. Note that the facets of a same tetrahedron may be glued together, and generalized triangulations are more general than simplicial complexes. The link of a vertex in T is the frontier of a closed regular neighborhood, and is itself a closed triangulated surface in the triangulation. If the link of a vertex v is a 2-sphere, we call v an *internal* vertex, otherwise (e.g., if the link is a torus), we call v an *ideal* vertex.

A 1-vertex ideal triangulation is a triangulation with exactly 1 ideal vertex, and no internal vertices. They represent non-compact 3-manifolds, that can be recovered from the 1-vertex

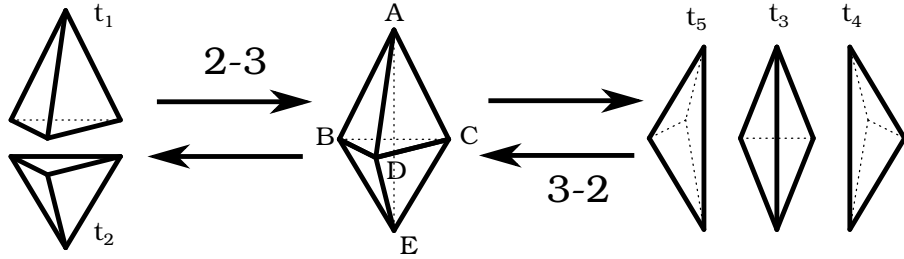


FIGURE 4. Illustration of the Pachner moves 2-3 and 3-2.

ideal triangulation by considering their realization where the vertex has been removed. Every knot complement can be represented by a 1-vertex ideal triangulation, where the link of the ideal vertex gives the frontier of a closed regular neighborhood of the knot. Intuitively, this is a triangulation of the sphere S^3 where the knot has been shrunk into a single point, distorting its neighborhood. Such 1-vertex ideal triangulation of a knot complement can be computed in polynomial time [6, 5].

Any two ideal triangulations of the same 3-manifold can be connected by a sequence of *Pachner moves* [11]. For 1-vertex ideal triangulations, they consist of the moves 2-3 and 3-2, inverse of each other, pictured in Figure 4.

2.2. Combinatorial description of hyperbolic geometry. Certain topological 3-manifolds can be equipped uniformly with a complete hyperbolic metric, which is unique up to isometry. They are called *hyperbolic manifolds*. They include the vast and important family of complements of *hyperbolic knots*.

We use the upper half-space model to represent the hyperbolic space \mathbb{H}^3 . This representation corresponds to $\{(z, r) | z \in \mathbb{C}, r \in \mathbb{R}_+^*\}$ with $\partial\mathbb{H}^3 = \mathbb{C} \cup \{\infty\}$ (from now on denoted $\partial\mathbb{H}^3$) consisting of the bottom plane $\mathbb{C} \times \{0\}$, together with the point at infinity, where geodesics are arcs of circles orthogonal to $\partial\mathbb{H}^3$. This model is *concordant*, *i.e.*, the measures of the angles in this model are the same as in the actual hyperbolic space.

An *ideal hyperbolic tetrahedron* is the convex hull of four distinct points of $\partial\mathbb{H}^3$. These points are the (ideal) vertices of the tetrahedron.

A vertex on $\partial\mathbb{H}^3$ is a vertex at infinity, thus it is not part of the tetrahedron. An example of ideal tetrahedron is shown in Figure 5. Up to isometry, the geometric shape of an ideal tetrahedron can be represented by a single complex number:

Definition 2.1 (Shape parameter). Given a ideal hyperbolic tetrahedron, there exists an isometry sending three of its vertices to 0, 1, and ∞ , and ensuring that the fourth vertex has positive imaginary part in the complex plane in $\partial\mathbb{H}^3 = \mathbb{C} \cup \{\infty\}$. The coordinate z of this fourth vertex is the *shape parameter* of the tetrahedron.

The shape parameter defines and illustrates the shape of a ideal tetrahedron. It depends on which vertices are sent to 0, 1, and ∞ . Other permutations of the vertices give the equivalent shape parameters $z' = \frac{z-1}{z}$ and $z'' = \frac{1}{1-z}$. The construction is well defined as isometries of \mathbb{H}^3 are determined by their action on three vertices of $\partial\mathbb{H}^3$.

Another way of characterizing the shape of a ideal hyperbolic tetrahedron is to consider its dihedral angles, *i.e.*, the angle formed by two faces meeting on a common edge ; see Figure 5. In an ideal tetrahedron, opposite angles are equal, and the sum of the six dihedral angles is

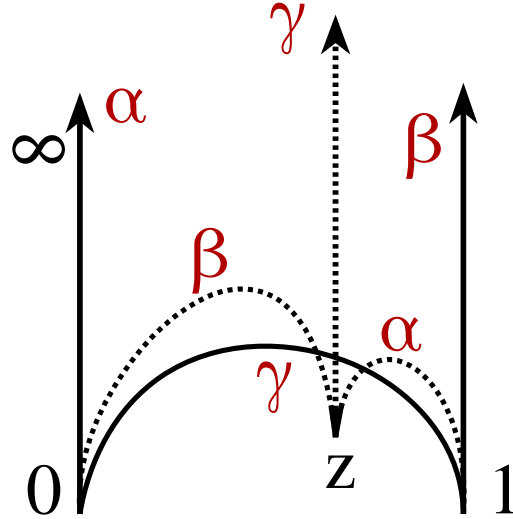


FIGURE 5. Ideal tetrahedron in the upper half-space model, the dihedral angles are denoted α , β and γ , the complex shape parameter z is associated to the edge between 0 and ∞ .

2π . We denote in the following the dihedral angles of a tetrahedron by a triplet (α, β, γ) with $2(\alpha + \beta + \gamma) = 2\pi$.

3. ANGLE STRUCTURES AND HYPERBOLIC VOLUME

In this section, we introduce notions connected to the computation of complete hyperbolic structures on triangulations via optimization methods. The approach given in this section is another formulation of Thurston's gluing equations, we refer the reader to [4, 13] for more details.

3.1. Linear equations and angle structures. Let T be a 1-vertex ideal triangulation of a knot complement M with n tetrahedra. Since opposite edges have same dihedral angles, all possible shapes of the tetrahedra can be represented by a vertex in \mathbb{R}^{3n} . We define an *angle structure*:

Definition 3.1 (Angle structures). Given an ideal triangulation T , an *angle structure* is a value assignment to the dihedral angles of the tetrahedra of T such that:

- (1) all the angles are strictly positive;
- (2) the three different dihedral angles of a tetrahedron sum to π ;
- (3) the dihedral angles around each edge of T sum to 2π .

The set of angle structures on T is denoted $\mathcal{A}(T)$.

Conditions 1 and 2 ensure the angles are in $(0, \pi)$ and that the tetrahedra are directly oriented. Condition 3 is necessary for points on the interior of edges to have a neighborhood isometric to a hyperbolic ball.

Constraints 1, 2, 3 are linear, hence the set $\mathcal{A}(T)$ of angle structures of a triangulation is a polytope in \mathbb{R}^{3n} of dimension $n + |\partial M|$ where $|\partial M|$ is the number of cusps of M ; in the case of knot complements, there is a single cusp. This *polytope* satisfies:

Theorem 3.2. (Casson; see [7]) *Let T be an ideal triangulation of M , an orientable 3-manifold with toric cusps. If $\mathcal{A}(T) \neq \emptyset$, then M admits a complete hyperbolic metric.*

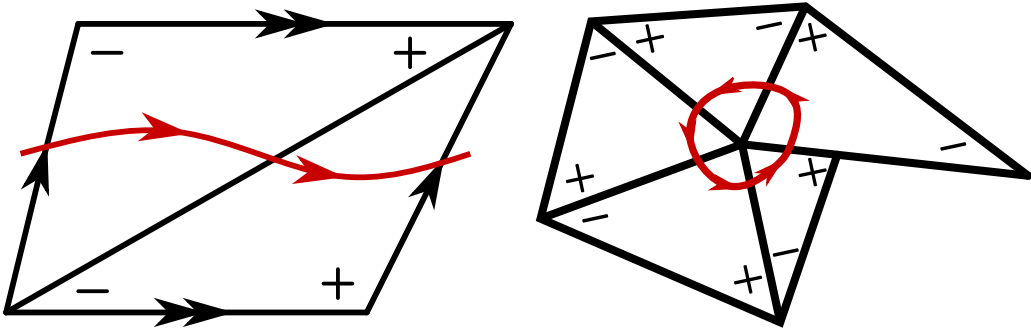


FIGURE 6. Left: leading (+) and trailing (−) corners associated to a closed normal curve on a torus. Right: an example of shearing singularity, angle structures do not prevent them and they forbid the presence of a CHS. A closed normal curve with associated leading and trailing corners is also displayed

Furthermore, a generating family for the tangent space of $\mathcal{A}(T)$ can be computed in polynomial time, using *leading-trailing* deformations, which are based on closed normal curves.

Definition 3.3 (Closed normal curve, Arc). Given a triangulated 2-dimensional orientable surface S , a closed normal curve on S is a closed curve on S such that its intersection with each triangle is either empty or a collection of disjoint segments joining distinct edges of the triangle. Such segments are called arcs.

Definition 3.4 (Leading-trailing deformations). Let T' be a triangulation of a 2-dimensional torus and σ an oriented closed normal curve on T' . Let n be the number of triangles of T' and \mathbb{R}^{3n} be a vector space of the values of the angles of the triangles. Given a directed arc in a triangle, the leading corner is the one opposed to the entering side of the segment, and the trailing is the one opposed to the exiting side.

Starting from $0 \in \mathbb{R}^{3n}$, and for each segment of σ , add 1 to the coordinate corresponding to the leading corner and subtract 1 to the coordinate corresponding to the trailing one. The resulting vector of \mathbb{R}^{3n} is the leading-trailing deformation associated to σ .

Figure 6 illustrates the leading (marked +) and trailing (marked −) corners associated to normal curves. In practice, in a 1-vertex ideal triangulation of a knot complement, T' will be the triangulated torus made of the intersection between T and the link of the ideal vertex. Let us consider the set B of vectors corresponding to the leading-trailing deformations of:

- one closed normal curve around each vertex of T' , see Figure 6 (Right);
- two normal curves generating the fundamental group of T' , see Figure 6 (Left).

Then we have:

Theorem 3.5 ([4]). B spans the tangent space of $\mathcal{A}(T)$.

3.2. Maximizing the hyperbolic volume. The hyperbolic volume of a ideal hyperbolic tetrahedra with dihedral angles $(a, b, c) \in (0, \pi)^3$ is given by the function vol :

$$\text{vol}(a, b, c) = L(a) + L(b) + L(c)$$

where L is the Lobachevsky function $L(x) = -\int_0^x \log |2 \sin t| dt$. The volume functional can be extended to the whole polytope $\mathcal{A}(T)$ by summing the volumes of the hyperbolic tetrahedra. The following result is due independently to Casson and Rivin.

Theorem 3.6 (Casson, Rivin[12]). *Let T be an ideal triangulation with n tetrahedra of M , an orientable 3-manifold with boundary consisting of tori. Then a point $p \in \mathcal{A}(T) \subset \mathbb{R}^{3n}$ corresponds to a complete hyperbolic metric on the interior of M if and only if p is a critical point of the function vol .*

Additionally, the volume functional is concave on $\mathcal{A}(T)$ and the maximum can be computed via convex optimization methods.

We can finally CHS that represent combinatorially complete hyperbolic metrics:

Definition 3.7 (Complete Hyperbolic Structure). A Complete Hyperbolic Structure (CHS) is a triangulation T equipped with an angle structure corresponding to the maximum of vol over $\mathcal{A}(T)$.

Remark 3.8. Angle structures are not CHS as they do not prevent shearing singularities, see Figure 6 (right), and consequently may represent *non-complete* hyperbolic metrics.

4. BEHAVIOR OF THE OPTIMIZATION

From the previous section, one can infer that finding algorithmically a CHS can be done by first finding a vertex inside the polytope $\mathcal{A}(T)$, then computing a basis of $\mathcal{A}(T)$, and then maximizing the (concave) hyperbolic volume on this subspace. If $\mathcal{A}(T) \neq \emptyset$ and the procedure finds the point maximizing the volume in the inside of the polytope, then the triangulation admits a complete hyperbolic structure represented by this point. Finally, if $\mathcal{A}(T) \neq \emptyset$ but the maximum of the volume functional is on the boundary, then one needs to re-triangulate the manifold in order to search for a triangulation admitting a CHS.

In this section, we study the outcome of the hyperbolic volume maximization on the space of angle structures. The result is given by the following lemma, which also appeared independently in [10]:

Lemma 4.1. *Let T be an ideal triangulation of M , a non-compact orientable 3-manifold with toric cusps. Let p be the point maximizing vol over $\overline{\mathcal{A}(T)}$, then at p , if a tetrahedron has an angle equal to 0, then all other angles of the tetrahedron are in $\{0, \pi\}$.*

In other words, either the maximization succeeds on the interior of $\mathcal{A}(T)$, or there is at least one tetrahedron with angles $(0, 0, \pi)$ in p . Such tetrahedron is called *flat*. It is not possible to have a tetrahedron with angles $(0, a, b)$, $(a, b) \in (0, \pi)$ in p .

Proof. Let $p = (p_1, p_2, p_3)$ be the angles (in $(0, \pi)$) of a tetrahedron and let $\vec{w} = (w_1, w_2, w_3)$ be the coefficients of a leading trailing deformation restricted to a single tetrahedron. Since inside the tetrahedron, the sum of the angles is constant, $w_3 = -(w_1 + w_2)$. We have, by the positivity of the sines:

$$(4.2) \quad -\frac{\partial \text{vol}(p)}{\partial \vec{w}} = \sum_{i=1}^3 -w_i \log \sin(p_i).$$

W.l.o.g., assume the maximization of the volume converges towards some point p where $p_1 = 0$ and $p_2 \leq p_3$.

If $p_2 > 0$, then $-w_1 \log \sin(p_1)$ is the only diverging member in 4.2. Note that we are converging towards p by following the vector \vec{w} , hence $p_1 = 0$ implies $w_1 \neq 0$. Thus p cannot be the limit of the optimal as the derivative of the volume diverges towards $-\infty$.

If $p_2 = 0$, then with $\lambda > 0$ and by using series developments:

$$-\frac{\partial \text{vol}(x, \lambda x, \pi - (\lambda + 1)x)}{\partial \vec{w}} = -\log \left(\frac{\sin(x)^{w_1} \sin(\lambda x)^{w_2}}{\sin((\lambda + 1)x)^{w_1 + w_2}} \right) \xrightarrow{x \rightarrow 0} -\log \left(\frac{\lambda^{w_2}}{(\lambda + 1)^{w_1 + w_2}} \right).$$

In this case, the different diverging members in 4.2 compensate each other.

Thus, the only possibility in order to converge on the boundary is to converge towards flat tetrahedra.

□

In consequence, we introduce in the next Section an algorithm that performs combinatorial modifications on a triangulation equipped with an angle structure, in order to get rid of flat tetrahedra.

5. COMBINATORIAL MODIFICATIONS OF TRIANGULATIONS

According to Lemma 4.1, the volume maximization either leads to a solution to the gluing equations, or to flat tetrahedra. In the latter case, the volume is still the maximum over the whole angle structure polytope. In this section, we discuss a method to get rid of flat tetrahedra by combinatorial modifications of the triangulation, while attempting to maintain the value of the volume functional, in order to push the maximization further.

This objective of maintaining the volume functional is done by geometric Pachner moves

5.1. Geometric Pachner moves. We perform Pachner moves on the triangulation that preserves the partial geometric data computed. More precisely, we define:

Definition 5.1 (Geometric Pachner move). A *geometric Pachner move* in an triangulation T with angle structure is a Pachner move in T such that the resulting triangulation admits an angle structure with identical dihedral angles for the tetrahedra not involved in the move. We say a tetrahedron is negatively oriented if one of its dihedral angle is negative.

Lemma 5.6 and 5.5 give the necessary and sufficient conditions to be able to perform geometric Pachner moves. When these conditions are met, Lemma 5.8 describes the computation of the angles of the new tetrahedra, its proof is left to Appendix B. To check if a geometric Pachner move can be done, it must be valid combinatorically, and it should be possible to assign dihedral angles to the new tetrahedra without altering the rest of the angle structure.

For Lemma 5.6 and 5.5, we refer to Figure 4 for illustration. We will define $t_1 = ABCD$ and $t_2 = BCDE$ two distinct tetrahedra glued along their common face, and $t_3 = ABCE$, $t_4 = ACDE$ and $t_5 = ADBE$ three distinct tetrahedra glued around their common edge. Assuming there is an underlying angle structure, let us denote $t(e)$ the value of the dihedral angle around the edge e in the tetrahedra t . Passing from (t_1, t_2) to (t_3, t_4, t_5) or the opposite without altering the rest of the angle structure will lead to the following equations:

$$(5.2) \quad t_1(BC) + t_2(BC) = t_3(BC), \quad t_1(CD) + t_2(CD) = t_4(CD), \quad t_1(DB) + t_2(DB) = t_5(DB)$$

$$(5.3) \quad t_1(AB) = t_3(AB) + t_5(AB), \quad t_1(AC) = t_3(AC) + t_4(AC), \quad t_1(AD) = t_4(AD) + t_5(AD)$$

$$(5.4) \quad t_2(EB) = t_3(EB) + t_5(EB), \quad t_2(EC) = t_3(EC) + t_4(EC), \quad t_2(ED) = t_4(ED) + t_5(ED)$$

Keeping in mind that the unknowns and the constant depends on which move is studied, and that by equality of the dihedral angles $t(UV) = t(XY)$ for $UVXY$ vertices of t , we have the following lemmas:

Lemma 5.5. *Let T be a triangulation with angle structure, let $t_3 = ABCE$, $t_4 = ACDE$ and $t_5 = ADBE$ be three distinct tetrahedra glued around an edge. A 3-2 geometric Pachner move can always be performed at AE .*

Proof. The 3-2 move is combinatorially valid as the resulting tetrahedra and their gluings are well defined. Let us have $t_1 = ABCD$ and $t_2 = BCDE$.

The system composed of Equations 5.2, 5.3 and 5.4 is linear with 6 unknowns: the dihedral angles of t_1 and t_2 . We need to check if this system admits a solution where the angles are in $(0, \pi)$. Note that as $t_3(AE)$, $t_4(AE)$, and $t_5(AE)$ are the angles around the edge AE , their sum is 2π .

$$\begin{aligned} t_1(AB) &= t_3(AB) + t_5(AB) &= 2\pi - (t_3(AE) + t_3(AC) + t_5(AE) + t_5(AD)) \\ &< 2\pi - (t_3(AE) + t_5(AE)) &= t_4(AE) \\ &< \pi \end{aligned}$$

$$t_1(AB) = t_3(AB) + t_5(AB) > 0$$

Thus, if the system admits a solution, the dihedral angles of t_1 and t_2 are in $(0, \pi)$ by symmetry.

Now let us check if all the equation can be satisfied. From Equation 5.3 and 5.4:

$$t_1(AC) + t_2(EC) = t_3(AC) + t_4(AC) + t_3(EC) + t_4(EC) = 2\pi - (t_3(AE) + t_4(AE)) = t_5(AE)$$

Thus the equations of Equation 5.2 are consequences of the other two. The system is linear with 6 independent equations and 6 unknowns, it admits a solution

Finally we have:

$$\begin{aligned} t_1(AB) + t_1(AC) + t_1(AD) &= t_3(AB) + t_5(AB) + t_3(AC) + t_4(AC) + t_4(AD) + t_5(AD) \\ &= 3\pi - (t_3(AE) + t_4(AE) + t_5(AE)) \\ &= \pi \end{aligned}$$

Thus the dihedral angles of t_1 sum to π , the same goes for t_2 by symmetry. And the move is always valid as long as we started with an angle structure. \square

Lemma 5.6. *Let T be a triangulation with angle structure, let $t_1 = ABCD$ and $t_2 = BCDE$ be two distinct tetrahedra glued along a face. A 2-3 geometric Pachner move can be performed at BCD if and only if $\forall e \in \{BC, CD, DB\}$, $t_1(e) + t_2(e) < \pi$.*

The proof uses similar arguments as above but is more involved. We postpone it to Appendix A.

Remark 5.7. In Lemma 5.6, several angle structure are possible after the move (for different values of λ , in the proof). Conversely, several angle structures lead to the same result for the 3-2 move. This is because angle structure are blind to shearing singularities, see Figure 6. If such a singularity exists, a 3-2 move can still be performed while maintaining the whole angle structure, but it will decrease the hyperbolic volume of the structure. It is due to the fact that the singularity, which maximized the volume, is fixed in the process.

Lemma 5.8. *There is an algorithm with constant number of arithmetic operations computing the shapes of the tetrahedra resulting from 2-3 and 3-2 moves.*

5.2. Getting rid of flat tetrahedra. Let T be a triangulation with an angle structure admitting a flat tetrahedron t , and (e, e') the associated edges with dihedral angle π . By Lemma 5.6, it is not possible to get rid of a tetrahedra with a geometric 2-3 move. Indeed,

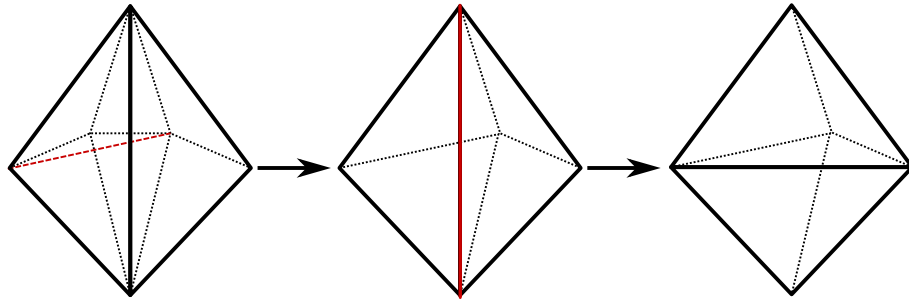


FIGURE 7. A sequence of moves getting rid of a flat tetrahedron. The bold vertical edge is contained in 4 tetrahedra, three of which are represented behind the edge. The fourth tetrahedron is implicit, situated at the front, and flat. First, create the red edge of the first drawing with a 2-3 move. Then delete the red edge of the second drawing with a 3-2 move. Finally, discard the flat tetrahedron.

if an edge of t has a dihedral angle equal to π , the second tetrahedron concerned by the 2-3 move must have a dihedral angle equal to 0, and consequently a 2-3 move will produce a flat tetrahedron (see Appendix B).

In order to get rid of t , our strategy is to turn either e or e' into an edge of degree three, at the center of three tetrahedra on which a 3-2 move can be performed (central edge of Figure 4, right). Note that edges of degree 2 prevent the existence of an angle structure as they force the two tetrahedra sharing the edge to be flat. As a consequence, we pre-process the triangulation with 2-3 moves to break these configurations. Consequently, all edges have degree at least 3, and our strategy is focus on *reducing* the incidence degree of angle π edges.

Basic move. Consider e an edge, the degree of which we want to reduce. The strategy is to perform 2-3 moves on the tetrahedra containing e , such that each move reduces the degree of the edge by one. Either for topological (tetrahedron glued to itself) or geometrical reasons, these moves will not always be possible, and the order in which they are done matters. This is described in Figure 7.

Remark 5.9. Doing a 2-3 move does not always reduce the degree of the edge, *e.g.*, when a tetrahedra is represented several times around an edge. However, doing a move that does not decrease the degree of the edge may delete the multiple occurrences of a tetrahedra around the edge and allow to continue with the simplification.

Remark 5.10. When a 2-3 move is performed around e , the dihedral angle of the new tetrahedron around e is equal to the sum of the previous two. Since the sum of the dihedral angles of a tetrahedron is equal to π , this means successfully reducing the degree of e may unlock previously forbidden moves.

Recursive moves. If no geometric Pachner is possible on an edge e , we attempt to reduce the degree of a nearby edge e_f , *i.e.*, an edge for which there exists a tetrahedra containing for e and e_f ; see Figure 8 (right) where e_f appears in blue. More precisely, let f be a triangle containing e such that the associated 2-3 move is forbidden for geometric reasons, then by Lemma 5.6 there is an edge e_f of f for which the associated dihedral angle is larger than π .

In consequence, reducing the degree of f to three without modifying the tetrahedra containing f and then performing a 3-2 move at f will reduce the degree of e by one; see Figure 8.

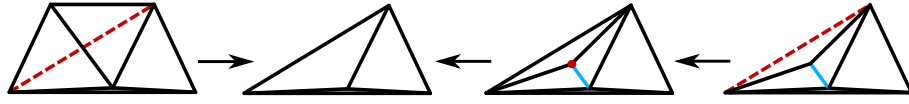


FIGURE 8. Two possible sequences of moves to reduce the degree of an edge, seen from above. The flat tetrahedron is at the bottom of the drawings. In the leftmost configuration, the geometric 2-3 move is possible and implements the first transformation of Figure 7. In the rightmost configuration, the geometric move is not possible; the algorithm consists of creating the tetrahedra with the red dashed edge, then to performing a 3-2 move on the central edge (with a red dot).

Algorithm 1 Reduction of the degree of an edge

```

1: procedure DECREASEDEG( $T, e$ )                                 $\triangleright$  An edge  $e$  of the triangulation  $T$ 
2:   for all  $f \in \text{STAR}(T, e)$  do                                 $\triangleright$  For all tetrahedra containing  $e$ 
3:      $T' \leftarrow \text{PACH}(T, f)$                                           $\triangleright$  New triangulation via Pachner moves
4:      $T'' \leftarrow \text{DECREASEDEG}(T', e)$                                  $\triangleright$  Recursive call
5:     if  $\text{DEG}(T'', e) == 3$  then
6:       return  $T''$ 
7:     end if
8:   end for
9:   return  $T$ 
10: end procedure

```

Note that in case a geometric Pachner move is not possible on e_f either, we call the procedure recursively in a neighborhood of e_f .

Remark 5.11. The choice of e_f in f is unique: it is not possible to have two dihedral angles larger than π ; selecting a move to reduce the degree of e boils down to selecting a triangle containing e .

The procedure is summarized in Algorithm 1. It consists of a tree-like backtracking search, each branch corresponding to a choice of 2-3 or 3-2 move to perform. This procedure is local and the number of moves performed depends on the degree of the edge to reduce; in particular it does not depend on the overall triangulation.

The procedure $\text{STAR}(T, e)$ returns all the triangles containing e . The procedure $\text{DEG}(T, e)$ counts the degree of e in T . The procedure $\text{PACH}(T, f)$ makes a 2-3 move if possible, tries to do a 3-2 otherwise (this would require additional calls to DECREASEDEG). A call to DECREASEDEG is followed by a 3-2 move to actually get rid of the flat tetrahedron.

5.3. Implementation details.

The implementation faces several practical challenges.

Breaking infinite loops. As such, the algorithm may loop infinitely on some instance, as 2-3 and 3-2 moves may reverse themselves. To counteract this phenomenon and avoid redundant modifications we store, at each modification, the *isomorphism signature* of the triangulation [2], characterizing uniquely the isomorphism type of the triangulation. This allows to recognize already processed triangulations and break branches of the backtracking algorithms. Note however that this makes the procedure no longer local.

Selecting the edge e . When attempting to remove a flat tetrahedron, one needs to choose between the two π -angled edges e and e' to reduce. In our implementation, we consider all dihedral angles of the edges e and e' (in the tetrahedra that contain them), and select the edge that has the larger smallest such angle. This performs better than a random choice.

Pruning the backtrack search. Some triangulations may have edges of large degree (more than 10), which produces wide search trees. Additionally, the recursive call to `DECREASEDEG` may induce trees of large depth. Experimentally, the better strategy consists of exploring exhaustively the first levels of the tree. We set the width of exploration to 8 and explore the first 2 levels of the search tree.

Order of Pachner moves. Different orders of Pachner moves leads to different triangulations. In practice, we favor 2-3 moves over moves 3-2, which performs best. Additionally, among the 2-3 moves performed to get rid of a flat tetrahedron containing edge e of angle π , we prioritize moves that eliminate tetrahedra for which e has a small dihedral angle. Among the 3-2, we used the same method as the one choosing between e and e' , indeed choosing a 3-2 boils down to choosing an edge to minimize its degree.

6. EXPERIMENTS

In this section, we study the experimental performance of our approach to find a triangulation with a CHS, and compare its performance with the software `SnapPy` [3]. `SnapPy` is the state-of-the-art software to study the geometric properties of knots and 3-manifolds, and is widely used in the low-dimensional topology community.

SnapPy. `SnapPy`'s method is based on a random re-triangulation followed by a simplification. The first step is constituted of $4n$ random 2-3 moves, where n is the number of tetrahedra in the triangulation. The simplification performs non-deterministic modifications to decrease the number of tetrahedra in the triangulation. Notably it removes some configurations that prevent angle structures from existing. The verification of the existence of a CHS is based on a especially tuned Newton method to solve the gluing equations. [14]

Unit of complexity, the *re-triangulation*. We compare the complexity of algorithms in number of *re-triangulations*. For `SnapPy`, one re-triangulation captures the entire set of $4n$ random 2-3 moves with the simplification. For our algorithm, a re-triangulation captures the set of geometric Pachner moves used to get rid of a single flat tetrahedron ; each re-triangulation requires a new call to the convex optimization. We also mention the number of necessary Pachner moves performed in order to find a triangulation with a CHS.

Data set. We apply our algorithms to the census of prime hyperbolic knots with up to 19 crossings. This census has been constituted by the efforts of many researchers in the field, and recently completed with the exhaustive enumeration of all knots with crossing number smaller than 19¹ [1].

For each knot, given by a knot diagram, we compute a triangulation of the knot complement using `Regina` [2], and simplify it with `SnapPy`. We then keep the triangulations admitting an angle structure but not a CHS, and hence require re-triangulation. They constitute the vast majority of the *Failure on first try* data of Table 1.

In our experiments, the knots are grouped by crossing numbers (form 14 to 19), and on whether they are alternating or not. Our experiments are run on the first 2500 knots of each

¹The census is available at <https://regina-normal.github.io/data.html>

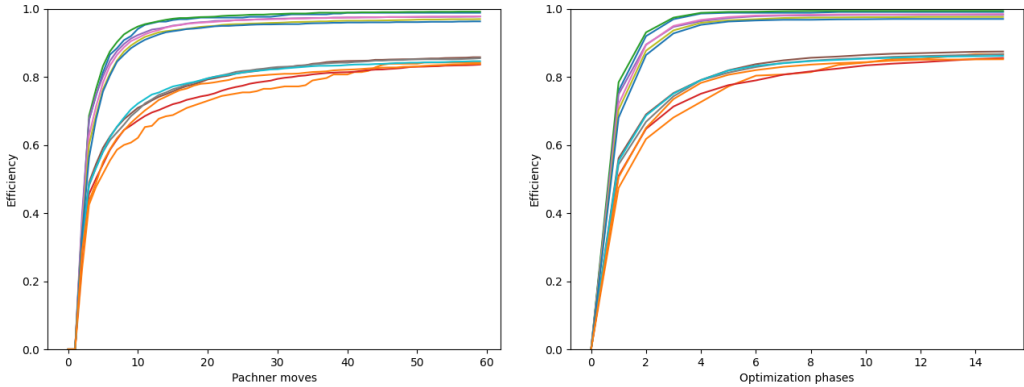


FIGURE 9. On the sample of triangulations, success rate in finding a CHS against the number of Pachner moves (left), and the number of optimization phases (right). The limit rate of success for alternating knots is 0.98, the limit rate for non-alternating knots is 0.87.

	# of optim phases					# of moves				
	1	2	3	4	5	2	3	4	10	30
Efficiency alter	0.73	0.89	0.95	0.97	0.97	0.36	0.63	0.72	0.92	0.97
Efficiency non-alter	0.53	0.67	0.74	0.78	0.81	0.30	0.47	0.52	0.70	0.81

FIGURE 10. Average of success rates for the alternating and non-alternating groups of knots.

of the 12 groups having an angle structure but no CHS. We also select a set of triangulations on which `SnapPy` requires more than 10 re-triangulation on average.

6.1. Efficiency of the method. Figure 9 represents the rate of knots on which our algorithm succeeds to find a triangulation with a CHS, for all the 12 groups of knots. It represents the success rate as a function of the number of Pachner moves (left), and as a function of the number of optimization steps. In both diagrams, the better success rate groups are the alternating knots.

While there is a significant difference between the efficiency on alternating and non-alternating knots, all the curves from both diagram have the same behavior: the first few optimization phases, or Pachner moves, are very effective.

Another important point is that, compared to the large number of moves done by `SnapPy` randomized re-triangulations and simplifications (linear in the overall number of tetrahedra of the triangulation), our method uses a much lower number of Pachner moves on average, as shown in Figure 10.

After the first few steps, the growth of the success rate slows down drastically. An interpretation of this phenomenon is that the tetrahedra created by the 2-3 moves tend to be more flat than the original ones. This leads to an increase in the number of required re-triangulation and issues with floating point arithmetic.

Limitations. It is to be noted that our method suffers from several phenomena: there are manifolds on which our method fails, the reasons to this being convergence problems because of the floating point arithmetic, the creation of flatter tetrahedra or the volume modification mentioned in Remark 5.7. Furthermore some triangulations have several very

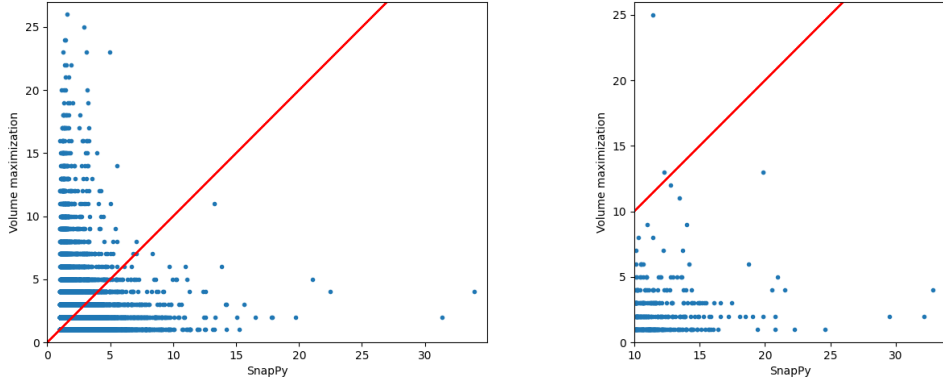


FIGURE 11. Number of re-triangulations required by our method over the number of re-triangulations required by `SnapPy` on the 12 groups of knots (left) and on the group of triangulations on which `SnapPy` requires more than 10 re-triangulations in average (right). Since our method is deterministic, the points have discrete ordinates. The diagonal $x = y$ appears in red.

high degree edges and looking for the correct sequence of geometric Pachner moves can exceed our timeout. We illustrate in the next section that is it however complementary to the state-of-the-art algorithms and can be used in conjunction with `SnapPy`.

6.2. Comparison with `SnapPy`. We compare in Figure 11 the average number of randomized re-triangulations required by `SnapPy` to find a triangulation with a CHS, and the (deterministic) number of re-triangulations of our method. The majority of the CHS are found within few re-triangulations on average. Both methods manage to find 78% of them in two steps. Since both methods are quite efficient on the majority of the triangulations, we use this measure to be able to find the cases that are well managed by one method, and not by the other.

Figure 11 compares the performance of both approaches in number of re-triangulations. It appears that the performance of the methods are substantially orthogonal: our methods performs rather poorly on knot complements for which `SnapPy` finds a triangulation with CHS rapidly (fewer than 5 re-triangulations), but our methods constitutes a substantial improvement on manifolds for which `SnapPy` struggles to find a solution. This phenomenon highlights the fact that the methods are complementary, and our approach handles hard cases much better. Since both methods are quite effective in general, we remind that the majority of the points are in the bottom left corner of the graph.

7. HYBRID ALGORITHM

In light of the previous results, we complement `SnapPy` with the geometric Pachner moves and resolution of flat tetrahedra techniques introduced in this article, into a hybrid algorithm.

`SnapPy` does not produce angle structures as defined in Section 3, as it constructs *negative tetrahedra*, i.e., tetrahedra whose shape has a negative imaginary part. Our hybrid method consists of calling `SnapPy` to randomize and simplify the triangulation, and, in case the triangulation admits only few negative tetrahedra (with low degree edges), call the resolution of flat tetrahedra with geometric Pachner moves of Section 5 on these negative tetrahedra. Loop until a CHS is found.

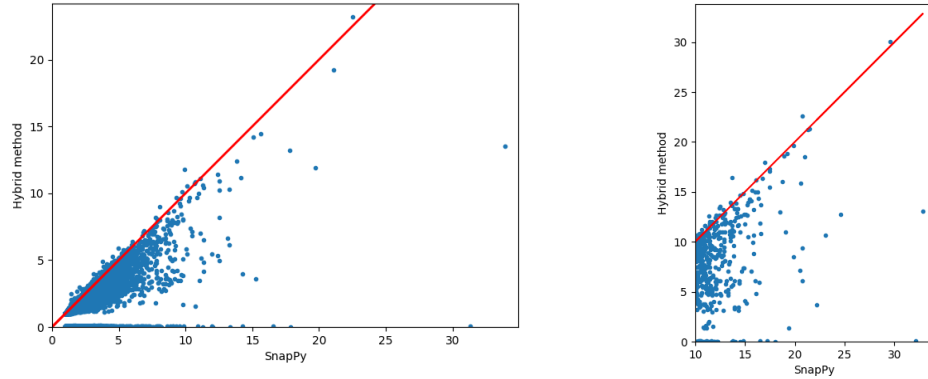


FIGURE 12. Number of re-triangulations required by the hybrid method against the number of re-triangulations of `SnapPy` alone, for the 12 groups of knots (left) and the group of triangulations requiring more than 10 re-triangulation on average (right). The points on the x axis correspond to the case where our heuristic found a CHS without requiring a re-triangulation.

The result of this method are summarized in Figure 12. With this simple idea we manage to never do worse than `SnapPy`, and on average we reduce the number of randomization by 40%. Note that because we are quite selective on the triangulation we apply our method on, the number of Pachner moves is quite low. The figure compares the number of re-triangulations (together with extra Pachner moves) of the hybrid method against the number of re-triangulations of `SnapPy` alone.

REFERENCES

- [1] Benjamin A. Burton. The Next 350 Million Knots. In Sergio Cabello and Danny Z. Chen, editors, *36th International Symposium on Computational Geometry (SoCG 2020)*, volume 164 of *Leibniz International Proceedings in Informatics (LIPIcs)*, pages 25:1–25:17, Dagstuhl, Germany, 2020. Schloss Dagstuhl–Leibniz-Zentrum für Informatik. URL: <https://drops.dagstuhl.de/opus/volltexte/2020/12183>, doi: 10.4230/LIPIcs.SoCG.2020.25.
- [2] Benjamin A. Burton, Ryan Budney, William Pettersson, et al. Regina: Software for low-dimensional topology. <http://regina-normal.github.io/>, 1999–2021.
- [3] Marc Culler, Nathan M. Dunfield, and Jeffrey R. Weeks. SnapPy, a computer program for studying the geometry and topology of 3-manifolds. <https://snappy.math.uic.edu/>, 1991–2021.
- [4] David Futer and François Guéritaud. From angled triangulations to hyperbolic structures, 2010. [arXiv: 1004.0440](https://arxiv.org/abs/1004.0440).
- [5] Joel Hass, Jeffrey C. Lagarias, and Nicholas Pippenger. The computational complexity of knot and link problems. *J. ACM*, 46(2):185–211, 1999. URL: <http://dx.doi.org/10.1145/301970.301971>, doi:10.1145/301970.301971.
- [6] William H. Jaco and J. Hyam Rubinstein. 0-efficient triangulations of 3-manifolds. *Journal of Differential Geometry*, 65:61–168, 2002.
- [7] Marc Lackenby. Word hyperbolic dehn surgery. *Inventiones mathematicae*, pages 243–282, 2000. doi: <https://doi.org/10.1007/s002220000047>.
- [8] George D. Mostow. *Strong Rigidity of Locally Symmetric Spaces*. Princeton University Press, 1973. URL: <https://doi.org/10.1515/9781400881833>, doi:doi:10.1515/9781400881833.
- [9] Hitoshi Murakami and Yoshiyuki Yokota. *Volume Conjecture for Knots*. Springer, 2018. doi:<https://doi.org/10.1007/978-981-13-1150-5>.
- [10] Barbara Nimershiem. Geometric triangulations of a family of hyperbolic 3-braids, 2021. [arXiv:2108.09349](https://arxiv.org/abs/2108.09349).

- [11] Udo Pachner. P.l. homeomorphic manifolds are equivalent by elementary shellings. *European Journal of Combinatorics*, 12(2):129–145, 1991. URL: <https://www.sciencedirect.com/science/article/pii/S0195669813800807>, doi:[https://doi.org/10.1016/S0195-6698\(13\)80080-7](https://doi.org/10.1016/S0195-6698(13)80080-7).
- [12] Igor Rivin. Euclidean structures on simplicial surfaces and hyperbolic volume. *Annals of Mathematics*, 139:553–580, 1994.
- [13] W. P. Thurston. *The geometry and topology of 3-manifolds*, volume 1. Princeton University Press, Princeton, N.J., 1980. Electronic version 1.1 - March 2002. URL: <http://library.msri.org/books/gt3m/>.
- [14] Jeffrey Weeks. Computation of hyperbolic structures in knot theory. *Handbook of Knot Theory*, 10 2003. doi:[10.1016/B978-044451452-3/50011-3](https://doi.org/10.1016/B978-044451452-3/50011-3).

APPENDIX A. PROOF OF LEMMA 5.6

Lemma A.1. *Let T be a triangulation with angle structure, let $t_1 = ABCD$ and $t_2 = BCDE$ be two distinct tetrahedra glued along a face. A 2-3 geometric Pachner move can be performed at BCD if and only if $\forall e \in \{BC, CD, DB\}$, $t_1(e) + t_2(e) < \pi$.*

The proof uses similar arguments as above but is more involved. We postpone it to Appendix A.

Proof. The 2-3 move is combinatorially valid as the resulting tetrahedra and their gluings are well defined. Let us have $t_3 = ABCE$, $t_4 = ACDE$ and $t_5 = ADBE$.

From Equations 5.2 we have that if $\exists e \in \{BC, CD, DB\}$, $t_1(e) + t_2(e) \geq \pi$ then one of the resulting tetrahedra will have a dihedral angle larger than π , preventing the validity of the move. Let us assume it is not the case.

The system composed of Equations 5.2, 5.3 and 5.4 is linear with 9 unknowns: the dihedral angles of t_3 , t_4 and t_5 . From Equations 5.2, the values of $t_3(AE)$, $t_4(AE)$, and $t_5(AE)$ are fixed and we have:

$$t_3(AE) + t_4(AE) + t_5(AE) = t_1(BC) + t_2(BC) + t_1(CD) + t_2(CD) + t_1(DB) + t_2(DB) = 2\pi$$

Thus the constraint around the edge AE is satisfied.

Summing the equations of Equation 5.3 on the one hand, and the equations of Equation 5.4 on the other hand both gives:

$$\pi = t_3(AB) + t_5(AB) + t_3(AC) + t_4(AC) + t_4(AD) + t_5(AD)$$

We also have that the sum of the dihedral angles of t_3 is π (and by symmetry it is true for t_4 and t_5):

$$\begin{aligned} t_3(AB) + t_3(AC) + t_3(AE) &= t_1(BC) + t_2(BC) + t_1(AB) + t_1(AC) - t_5(AB) - t_4(AC) \\ &= t_1(BC) + t_1(AB) + t_1(AC) + t_2(BC) - t_2(ED) \\ &= \pi \end{aligned}$$

Now, let us note that fixing any unknown fixes the values of the others, thus the system has exactly one degree of freedom: if $(t_3(AB), t_3(AC), t_4(AC), t_4(AD), t_5(AD), t_5(AB))$ is a solution to the system, then for any $\lambda \in \mathbb{R}$, $(t_3(AB) + \lambda, t_3(AC) - \lambda, t_4(AC) + \lambda, t_4(AD) - \lambda, t_5(AD) + \lambda, t_5(AB) - \lambda)$ is also a solution. This is discussed in Remark 5.7. We denote by Λ_+ the set of dihedral angle for which λ is added, and Λ_- the complement.

The last step of the proof is to show that there exists a choice of λ such that all the dihedral angles are positive, given that the dihedral angles of the tetrahedra sum to π is enough to have them in $(0, \pi)$.

By Lemma A.2, there is always a choice of dihedral angle such that fixing it to 0 ensures that the elements of Λ_+ are positive and those of Λ_- are non negative (or Λ_- and Λ_+ respectively, depending on whether the selected angle is in Λ_+ or Λ_-). If the elements of Λ_+ positive, then picking a sufficiently small negative λ to modify the dihedral angles will maintain the elements of Λ_+ positive, and will turn positive those of Λ_- , in the other case, in the same way a small positive λ will ensure the positivity of all the angles.

Thus there exists an angle structure corresponding to and coherent with the result of the Pachner move. \square

Lemma A.2. *With the notations and the assumption of the proof of Lemma 5.6, there is always a choice of dihedral angle x in $\{t_3(AB), t_3(AC), t_4(AC), t_4(AD), t_5(AB), t_5(AD)\}$ such that fixing $x = 0$ leads to the elements of Λ_+ being positive and those of Λ_- being non negative (or Λ_- and Λ_+ respectively).*

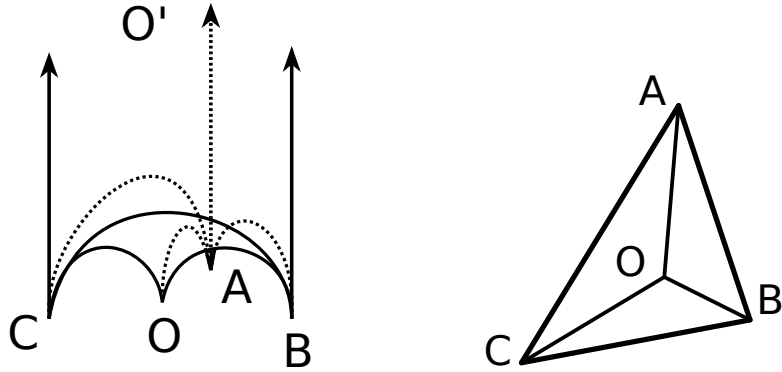


FIGURE 13. Left: disposition of the five vertices that admits two triangulations linked by a Pachner move in the hyperbolic space. Right: disposition of the vertices on $\partial\mathbb{H}^3$.

Proof. Let us assume the Lemma is false.

If $t_3(AC)$ is set to 0, then $t_3(AB) = \pi - t_3(AE) > 0$, $t_5(EB) = t_2(EB) > 0$ and $t_4(ED) = t_1(AC) > 0$. Furthermore $t_4(AD) = \pi - (t_4(AC) + t_4(AE)) = t_1(AD) - t_2(EB)$ and $t_5(AB) = t_2(ED) - t_1(AC)$. Note that the elements of Λ_+ are positive and the elements of Λ_- are non-negative if $t_4(AD)$ and $t_5(AB)$ are non-negative. Let us assume $t_1(AD) - t_2(EB) < 0$.

If $t_4(AD)$ is set to 0, like previously the elements of Λ_+ are positive, and $t_3(AC) = t_2(EB) - t_1(AD) > 0$ and $t_5(AB) = t_1(AB) - t_2(EC)$. If the lemma is false, then $t_1(AB) - t_2(EC) < 0$.

If $t_5(AB)$ is set to 0, like previously the elements of Λ_+ are positive, and $t_3(AC) = t_1(AC) - t_2(ED)$ and $t_4(AD) = t_2(EC) - t_1(AB) < 0$. If the lemma is false, then $t_1(AC) - t_2(ED) < 0$.

The previous deductions give $t_1(AB) + t_1(AC) + t_1(AD) < t_2(EB) + t_2(EC) + t_2(ED)$, which is absurd as these two sums are equal to π . The assumption that $t_1(AD) - t_2(EB) < 0$ must be false, and by symmetry $t_2(ED) - t_1(AC) < 0$ will be false too.

This is absurd and the Lemma is true. □

APPENDIX B. GEOMETRIC PACHNER MOVES

Section 5 introduces the geometric Pachner moves, this section provides the dihedral angles of the resulting tetrahedra depending on the initial ones.

B.1. Framework. In the upper half-space we consider the following: let A , B , C , O and O' be ideal vertices, O' is at the infinity, A , B and C are on the boundary plane and O in on the plane, inside the Euclidean triangle defined by A , B and C , see Figure 14. There are two sets of well defined tetrahedra: on the one hand the set β composed by $ABCO$ and $ABCO'$ and on the other hand the set γ composed by $ABOO'$, $BCOO'$ and $CAOO'$. These two sets are the image one of the other by a Pachner move. Given the dihedral angles of the tetrahedra in one set, we want to compute the dihedral angles for the other set. Since the model used is conformal, the computations can be boiled down to a problem in Euclidean geometry:

- The dihedral angles of $ABOO'$ can be read on the triangle ABO , and the same goes for $BCOO'$ and $CAOO'$ with BCO and CAO respectively.
- The dihedral angles of $ABCO'$ corresponds to the angles of ABC .
- The angle \widehat{AOB} is the sum of the dihedral angles around OC in $ABCO$ and $O'C$ in $ABCO'$, and same relations exist for \widehat{AOC} and \widehat{BOC} .

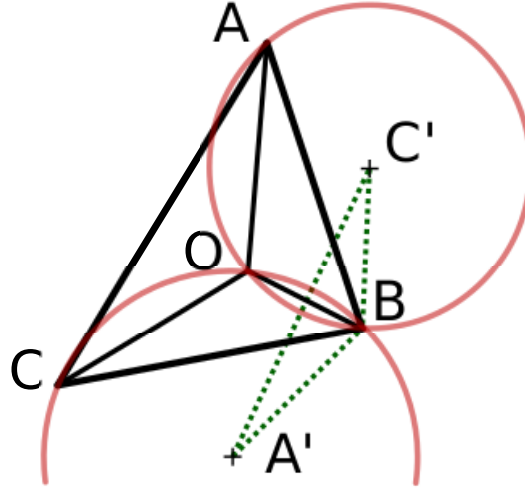


FIGURE 14. Drawing of the construction to compute the dihedral angles after a 2-3 move. The circles in red of center C' and A' are the circumcircles of respectively ABO and BCO .

Remark B.1. The correspondence between the angles of the tetrahedra and the angles of the triangles comes from the fact that the hyperbolic planes that go through O' are represented by straight Euclidean planes orthogonal to the plane of A, B, C and O . The relations with the angles of $ABCO$ comes from the equality between the angles around OO' and the angles formed by the two tetrahedra in the hyperbolic space.

Remark B.2. In this section, O is taken inside ABC . When O is outside, the set of the three tetrahedra can have negatively oriented members: the geodesic between O and O' does not pass through the hyperbolic face defined by A, B and C . This is also the case for the set of two tetrahedra when O is outside the circumcircle of ABC in the boundary plane.

The problem of computing the dihedral angles after a Pachner move is then equivalent to the following:

- For the 32 move given the angles of ABO , ACO and BCO , compute the angles of ABC and the angles around O .
- For the 23 move given the angles of ABC and the angles around O , compute the angles of ABO , ACO and BCO .

B.2. Analysis of the 32 move. The values of the angles around O are already known and the angles of ABC are the sum of two angles, e.g. $\widehat{ABC} = \widehat{ABO} + \widehat{OBC}$.

B.3. Analysis of the 23 move. Let us consider (C', r_c) the circumcircle of ABO and (A', r_a) the circumcircle of BCO . Then:

By the law of sines, $r_c = AB \frac{\sin(\widehat{C'BA})}{\sin(\widehat{AC'B})}$.

$AC'B$ being isosceles, $\widehat{C'BA} = (\pi - \widehat{AC'B})/2$, and by the inscribed angle theorem $2\pi - \widehat{AC'B} = 2\widehat{AOB}$. Thus $\widehat{C'BA} = \widehat{AOB} - \pi/2$.

$$\sin(\widehat{C'BA}) = \sin(\widehat{AOB} - \pi/2) = -\cos(\widehat{AOB})$$

$$\sin(\widehat{AC'B}) = \sin(2\pi - \widehat{AOB}) = -\sin(\widehat{AOB})$$

$$\text{Hence } r_c = AB \frac{\cos(\widehat{AOB})}{\sin(2\widehat{AOB})} = \frac{AB}{2\sin(\widehat{AOB})}.$$

$$\text{Likewise } r_a = \frac{CB}{2\sin(\widehat{COB})}.$$

$$\text{By the law of sines } \frac{AB}{CB} = \frac{\sin(\widehat{ACB})}{\sin(\widehat{BAC})}.$$

$$r := \frac{r_c}{r_a} = \frac{\sin(\widehat{ACB}) \sin(\widehat{COB})}{\sin(\widehat{BAC}) \sin(\widehat{AOB})}$$

$$\widehat{C'BA'} = \widehat{C'BA} + \widehat{ABC} + \widehat{CBA'} = \pi + \widehat{ABC} - \widehat{AOC}$$

By the law of cosines in $A'C'B$:

$$\frac{r_a}{A'C'} = \frac{1}{\sqrt{1+r^2-2r \cos(\widehat{C'BA'})}}$$

$$\frac{r_c}{A'C'} = \frac{1}{\sqrt{1+r^{-2}-2r^{-1} \cos(\widehat{C'BA'})}}$$

By the law of sines:

$$\sin(\widehat{BC'A'}) = \frac{r_a}{A'C'} * \sin(\widehat{C'BA'})$$

$$\sin(\widehat{BA'C'}) = \frac{r_c}{A'C'} * \sin(\widehat{C'BA'})$$

To compute all the angles, we need the value of $\widehat{BC'A'}$. Since the value of $\sin(\widehat{BC'A'})$, $\sin(\widehat{BA'C'})$ and $\widehat{C'BA'}$ are known, the value of $\widehat{BC'A'}$ can be deduced without ambiguity.

Finally:

$$\begin{aligned} \widehat{ABO} &= \widehat{C'BO} - \widehat{C'BA} \\ &= (\pi/2 - \widehat{BC'A'}) - (\widehat{AOB} - \pi/2) \\ &= \pi - (\widehat{BC'A'} + \widehat{AOB}) \end{aligned}$$

All the elements of the last line are known, thus \widehat{ABO} can be computed and all the other angles can be deduced from here.